FULL PAPER

Supramolecular Motifs in s-Block Metal-Bound Sulfonated Monoazo Dyes, Part 1: Structural Class Controlled by Cation Type and Modulated by Sulfonate Aryl Ring Position

Alan R. Kennedy,*[a] Jennifer B. A. Kirkhouse,[a] Karen M. McCarney,[a] Olivier Puissegur,[a] W. Ewen Smith,[a] Edward Staunton,[a] Simon J. Teat,[b] Julian C. Cherryman,[c] and Rachel James[c]

Abstract: The solid-state structures of 43 Li, Na, K, Rb, Mg, Ca and Ba salts of *para*- and *meta*-sulfonated azo dyes have been examined and can be categorised into three structural classes. All form alternating organic and inorganic layers, however, the nature of the coordination network that forms these layers differs from class to class. The class of structure formed was found to be primarily governed by metal type, but can also be influenced by the nature and position of the organic substituents. Thus, for the *para*-sulfonated azo dyes, Mg compounds form solvent-separated ion-pair solids; Ca, Ba and Li compounds form simple coordination networks based on metal–sulfonate bonding; and Na, K and Rb compounds form more complex, higher dimensional coordination networks. Compounds of *meta*-sulfonated azo dyes follow a similar pattern, but here, Ca species may also form solvent-separated ion-pair solids. Significantly, this first attempt to classify such dyestuffs using the principles of supramolecular chemistry succeeds not only for the simple dyes used here as model compounds, but also for more complex molecules, similar to modern colourants.

Keywords: alkali metals · alkaline earth metals · coordination frameworks · dyes/pigments · sulfonate ligands

Introduction

Most studies of solid-state metal–organic coordination networks are concerned with the design of complex new materials through understanding and exploiting the predictable supramolecular behaviour of simple fragments—a technique widely referred to as crystal engineering. This paper, however, attempts to rationalise the behaviour of a motif (the metal–sulfonate bond) that is highly variable and unpredictable, but which is common in compounds, for example, many azo colourants, already of interest in materials science.

Our overall aim was to elucidate the sulfonate's supramolecular motifs, to link these motifs to physical properties and thereby perform chemical modifications to improve the performance of the dyestuffs. Such developments are of interest in two specific areas: Firstly, the s-block metal complexes of sulfonated azo colourants are of general interest to structural chemists, as they exemplify the role of such metals in forming polymeric coordination networks.[1] Studies on s-block supramolecular systems are still relatively uncommon,[2] compared to similar work using transition metals as supramolecular building blocks.[3] Secondly, the structures of these compounds are of specific interest to the dye and pigment industries, as many of the materials' commercially significant properties (solubility, habit, stability and even colour) are dependent on or are influenced by their solid-state structure.[4]

Correlating crystal structure to properties is fundamental to the pigment industry, where the colourant is typically used as a crystalline dispersion in the material to be coloured, but it is also of importance in the manufacturing process of both dyes and pigments, for which properties such as solubility and habit must be taken into account. Similarly, the pharmaceuticals industry has recognised the importance of structure–property relationships for some

[a] Dr. A. R. Kennedy, J. B. A. Kirkhouse, K. M. McCarney,
O. Puissegur, Prof. W. E. Smith, E. Staunton
Department of Pure & Applied Chemistry
University of Strathclyde
Glasgow G1 1XL (Scotland)
Fax: (+44) 141-552-0876
E-mail: a.r.kennedy@strath.ac.uk

[b] Dr. S. J. Teat
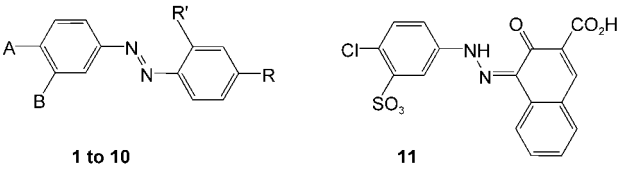CCLRC Daresbury Laboratory
Warrington WA4 4AD (England)

[c] Dr. J. C. Cherryman, Dr. R. James
Avecia Ltd, PO Box 42, Hexagon House
Blackley, Manchester M9 8ZS (England)

time,[5] as well as that elucidating the molecular–recognition properties of molecules is important as this provides insight into the binding behaviour of molecules of substrates. It can be argued that this is equally as relevant to dye–substrate interactions as it is to biological systems. In fact, much of the limited structural work to date on sulfonated azo dyes has originated from the bioscience community, and concerns the investigation of the modes of binding of sulfonated azo dyes to biomolecules.[6]

The dearth of sulfonated azo structures relevant to the colourants industry is due to a combination of perceived and genuine difficulties in examining such structures. In general, the role of s-block metals in forming supramolecular motifs has been neglected in favour of studying transition metals. The rationale behind this being that the increased variability of s-block metals' coordination geometry and their lack of intrinsically useful properties (i.e., magnetism or variable oxidation states) might appear to make them less interesting. However, s-block metals do have some advantages for application in materials science; they are non-toxic, cheap and generally amenable to aqueous preparation. For these reasons, s-block salts are the preferred formulations for a host of commercial materials, including many common pharmaceuticals and colourants. Similarly, sulfonates have been largely ignored by structural chemists in favour of the analogous phosphates, as sulfonates are generally weaker ligands with more variable coordination modes.[7] A genuine experimental difficulty in examining salts of sulfonated azo dyes that are commonly used in the colourants industry is that they have notoriously poor crystal growth properties. Commercial pigments are by design highly insoluble, making it difficult to grow the high quality crystals needed for single-crystal diffraction. Even the more soluble and thus tractable dyes form either amorphous solids or crystals with highly anisotropic habits and multiple defects. Thus, despite their widespread occurrence, little is known of the solid-state structures of these compounds and even less about their structure–property relationships.

To correlate the structures of sulfonated azo colourants to their physical properties, it is first necessary to characterise a suitable family of closely related structures accurately enough to allow elucidation of any common structural themes. The difficulty in crystallising commercial colourants means that, whilst individual structures may eventually be obtained,[8] producing a series of closely related structures is prohibitively difficult and time-consuming. Our approach was to investigate simple model dyes (see Table 1) that have enhanced crystallinity whilst retaining the same functional or molecular recognition groups as their more complex, commercial relatives. Such compounds have previously been used as model dyes in a wide variety of studies.[9] Initial results[1] on Na and Ca compounds showed that para-sulfonated monoazo dyes do have a tendency to form polymeric coordination arrays. Some generalizations could be made with respect to the metal coordination geometries found, the roles of the different azo substituents (SO_3^-, OH and NH_2) and the role of water ligands. However, this initial work also revealed the inherent variability of these systems and the inability to satisfactorily categorise them using the limited

Table 1. Sulfonated azo anions investigated.

Ligand no.	A	B	R	R'
1	SO_3	H	OH	H
2	SO_3	H	OH	OH
3	SO_3	H	NH_2	H
4	SO_3	H	NMe_2	H
5	SO_3	H	$N(CH_2CH_2OH)_2$	H
6	SO_3	H	OH	Me
7	SO_3	H	NEt_2	H
8	H	SO_3	OH	H
9	H	SO_3	OH	OH
10	H	SO_3	$N(CH_2CH_2OH)_2$	H

data available. All the arrays examined were unique, with zero-, one-, two- and three-dimensional coordination networks represented and no consistency in the coordination mode of the sulfonate groups. On the simplest level, the inorganic metal–ligand framework appeared to determine the structure, but simply changing the substituent on the organic dye from OH to NH_2 fundamentally altered the metal coordination and subsequently the array formed. This paper reports the extension of the previous work to Li, Na, K, Rb, Mg, Ca and Ba salts of the range of simple para- and meta-sulfonated azo dyes shown in Table 1. The structures of these compounds are discussed, we propose categorisation into three classes and examine how metal type and organic substitution control structural class. Finally, we demonstrate how the classification rules derived from the simple model dyes can be applied to more complex colourants.

Results and Discussion

Sample preparation and methodology: All azo species shown in Table 1 were synthesised via diazonium salts by using standard coupling techniques.[10] Initially, the Na salts of the dyes were isolated (except for **6** which gave the free acid form) and these were then transformed into the range of salts required by aqueous treatment with excess of the appropriate metal halide or hydroxide. Samples suitable for single-crystal analysis, by using either conventional laboratory techniques or synchrotron radiation,[11] were grown by recrystallisation from water by using simple, slow cooling or evaporation techniques. No attempt was made to control pH during the recrystallisation stage. Together with the six known literature examples,[1,12] this gave a dataset of 43 known single-crystal structures of s-block metal salts of simple para- or meta-sulfonated azo dyes (see Table 2). For reasons of simplicity and space, a subset of only 12 of the new structures has been selected to illustrate the points made herein and these structures are presented in full. However, any general structural points made are true for all known structures. Differential Scanning Calorimetry (DSC)

Table 2. Categorisation and structural characteristics of s-block metal-sulfonated azo dye complexes.

	p-Sulfonated azo dyes	m-Sulfonated azo dyes	Bonding characteristics	Dimensionality of coordination network[a]
class 1: solvent-separated ions	**Mg1 Mg2 Mg3 Mg5 Na4**	**Mg8 Ca8 Ca9**	no SO₃–metal bonds	0
class 2: simple complexes	**Li2 Li3** *Li5* **Li6 Ca1 Ca1′ Ca2 Ca2′ Ca3 Ca4** *Ca5* **Ba3**	*Li8* **Ca10 Ca11** *Ba8*	SO₃–metal bonds, bound water is terminal	0 or 1
class 3: higher connectivity complexes	**Na1 Na2** *Na3* **Na4′ Na4″** *Na5 Na6* **Na7** *K1* **K2 K3 K5 K6** *Rb1* **Rb3**	*Na8 Na11 K8 Rb8*	SO₃–metal bonds, bridging always present, bound water bridges	0 or 1 or 2

[a] Dimensionality of the SO₃/metal/solvent coordination network. The complexes indicated by italics also propagate through bonding of a second functional group (OH or NH₂). This is discussed in the forthcoming paper forming Part 2 of this work.

and powder-diffraction techniques have been used to check for polymorphism. Those cases found are discussed below, but as a full polymorph screen has not been attempted, the existence of others is entirely possible. Certainly the hydrate forms lose water on heating and so anhydrous forms can be easily prepared.

Structural type 1, solvent-separated ion-pair solids: All 43 Li, Na, K, Rb, Mg, Ca and Ba structures investigated form layered structures with alternating organic and inorganic zones (Figure 1). This is strongly reminiscent of the well-
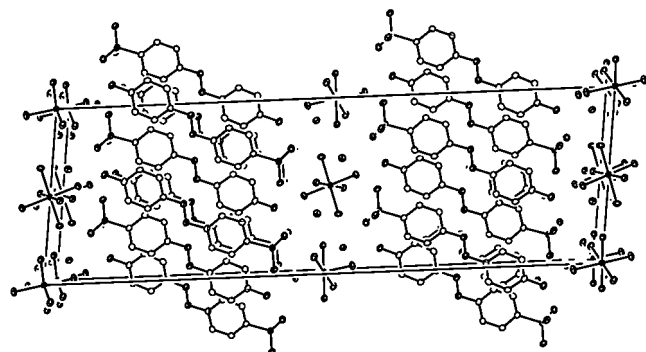

Figure 1. Packing diagram showing the alternating organic–inorganic layers in the structure of **Mg1**. These layers are common to all the structures discussed herein.

known organic–inorganic layer structures of metal phosphonates[13] and is consistent with previous work on s-block metal organic–sulfonate networks, in which this structural feature has been used to facilitate the inclusion of small molecules.[6e,7] The construction of these layers in each compound is, however, very different. The simplest structures, and the easiest to differentiate into a separate category, are those that form solvent-separated ion pairs. Here, the anticipated interaction between M and SO₃ does not occur, with the metal preferring to form exclusively ion–dipole interactions with water (or ROH). All the Mg structures examined fall into this category. Figures 1 and 2 show the structures of **Mg1** and **Mg8**, respectively, which are typical in that they consist of $[Mg(OH_2)_6]^{2+}$ ions that interact with the sulfonat-
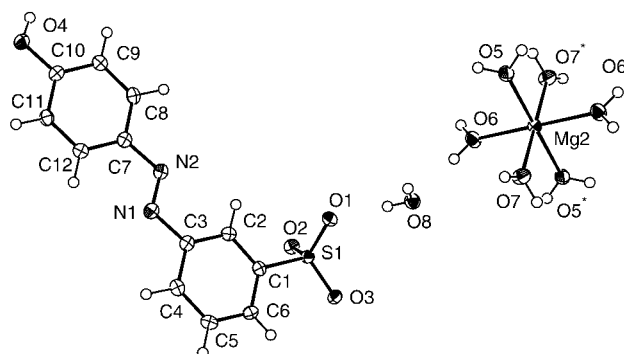

Figure 2. Solvent-separated ion-pair structure of **Mg8** showing the atom numbering adopted throughout for the azo anions.

ed azo anions exclusively through hydrogen bonding. These are, therefore, zero-dimensional coordination networks. Similar hexaaquamagnesium ion structures have been reported recently for other organic sulfonates, especially by Shimizu and co-workers.[7a,14]

Consideration of the fundamental properties underlying the ligand-bonding properties of s-block metals (electronegativity, charge and size) may indicate why Mg differs from the other metals investigated. As the most electronegative metal investigated, Mg–ligand bonds have a higher covalent contribution than the others, whilst as the smallest Group 2 ion, the higher charge density on Mg^{2+} means that it tends to make stronger interactions with Lewis bases. It is known that Mg−OH₂ bonds are considerably more stable than the other M−OH₂ bonds considered here.[15] Crystallisation from aqueous solution is in effect a competition reaction between the labile, charged sulfonate ligands and neutral water; the higher covalent nature of magnesium thus appears to favour direct hydration of the metal over interaction with the formally charged sulfonate group.

Structural type 2, simple M−SO₃ bonded complexes: Moving down Group 2 to the larger, more ionic and less electronegative metals Ca and Ba restores the expected M−SO₃ bonding motif.[1] For Ca, this may result in simple zero-dimensional, monometallic $[Ca(azo)_2(OH_2)_x]$ species (for azo = **1**, **3**, **4** or **10**), in which both the sulfonated azo and the

water ligands act as terminal and not bridging ligands (see Figure 3 for **Ca10** or reference [1] for **Ca3**). More commonly, the sulfonate group acts as a bridge between metal ions leading to simple one-dimensional chains. **Ca2** is a typical example (Figure 4). Here the coordination chain is propa-
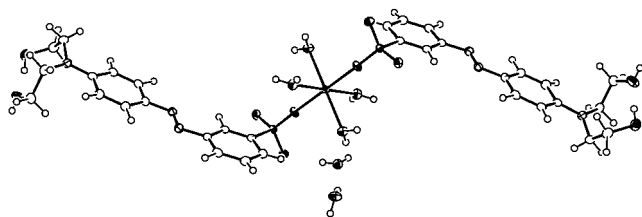

Figure 3. **Ca10** adopts a discrete, monometallic structure with the minimum of metal–sulfonate bonds.
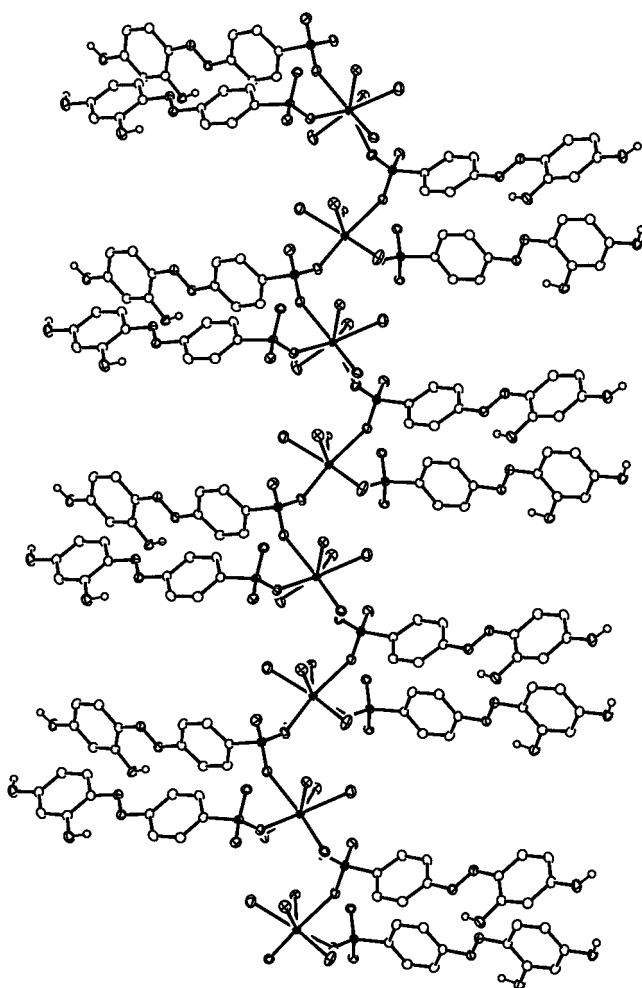

Figure 4. Simple one-dimensional chain structure of **Ca2**.

gated in the crystallographic *b* direction by η^2,μ_2-SO$_3$ bridges. A second azo ligand acts in a terminal η^1,μ_1-mode and the Ca coordination geometry is completed by five terminal H$_2$O molecules. Both **Ca1**[1] and **Ca2** have been isolated as both zero- and one-dimensional polymorphs. The structure of **Ba3** (Figure 5) illustrates how these species can have similar gross features, but differ markedly in detail. In
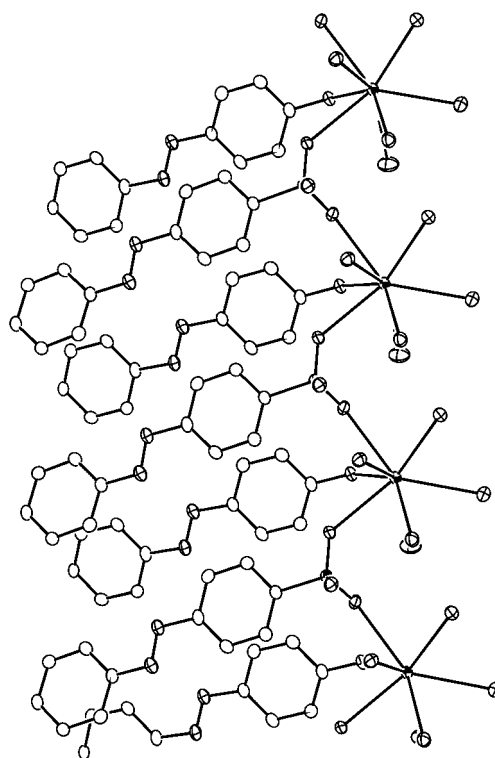

Figure 5. The chain structure of **Ba3** has two chemically distinct azo ligands. One bridges between metals through its sulfonate group, whilst the other bonds through its NH$_2$ tail.
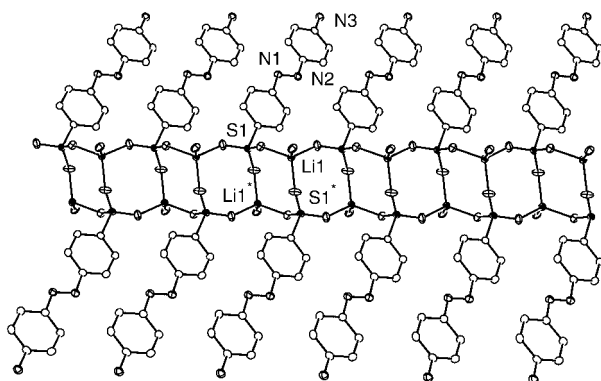
Ba3 a chain similar to that of **Ca2** is formed by means of the same SO$_3$ bridging mode, but here the terminal azo ligand bonds through its NH$_2$ tail and not through its SO$_3$ group, which is left to form hydrogen-bonding interactions only. Other differences are that the number of water ligands has increased to six and, more interestingly, that all the azo ligands lie solely on one side of the chain, giving it hydrophobic and hydrophilic faces. The relative simplicity of these structures arises from the fact that in the Ca and Ba species, the SO$_3$ unit does not form bridges to more than two metal atoms and does not use all three of its oxygen atoms to bind to the metal atoms (Table 3).

The Li species investigated also form networks based on simple chains. They differ from the Ca and Ba examples in that all are based on lithium's favoured tetrahedral coordination geometry and so have fewer coordinated water molecules. Some Li structures also display an increase in metal-bridging behaviour. Figure 6 shows the structure of **Li3**, which forms a ladder structure through η^3,μ_3-SO$_3$ bridges. The ladder motif is based on threefold nodes and is often seen in Li–amide chemistry, in which one Li coordination site is terminal.[16] In **Li3** both the sulfonate group and Li are tetrahedral centres, with one site blocked to polymer formation. A non-planar ladder is, therefore, an evident supramolecular motif for such species. The individual one-dimensional chains observed for Ca, Ba and Li are linked by both hydrogen bonding from one inorganic/hydroscopic chain to another (thus forming inorganic sheets linked by water–water and water–SO$_3$ interactions) and by hydrogen bonding from the OH or NH$_2$ dye "tails" of one chain to

Table 3. Metal coordination characteristics for complexes of **1** to **11**.

Metal	Electro-negativity[a]	Polariz-ability[b]	η[c] range	μ[c] range	Bound H₂O[d]	Coord. no. range	M–O distance range [Å][e]
Mg	1.293	0.094	0	0	6	6	2.041–2.091
Ca	1.034	0.47	0–2	0–2	2–7	6–8	2.270–2.717
Ba	0.881	1.55	0–2	0–2	5–6	9	2.696–2.979
Li	0.912	0.029	1–3	1–3	0–2	4	1.880–1.976
Na	0.869	0.179	0–3	0–5	0–4	4–6	2.258–2.706
K	0.734	0.83	2–3	1–4	0–2	7–9	2.608–3.202
Rb	0.706	1.40	3	5	0–1.5	7–8	2.817–3.232

[a] Configuration energy in Pauling units, from reference [20]. [b] 10^{-24} cm³, from reference [21]. [c] η and μ values are the number of O atoms of each SO₃ group used in bonding and the number of metal atoms bonded by each SO₃ group, respectively, as per reference [7a]. [d] Number per metal atom. [e] No other contacts less than 3.5 Å.

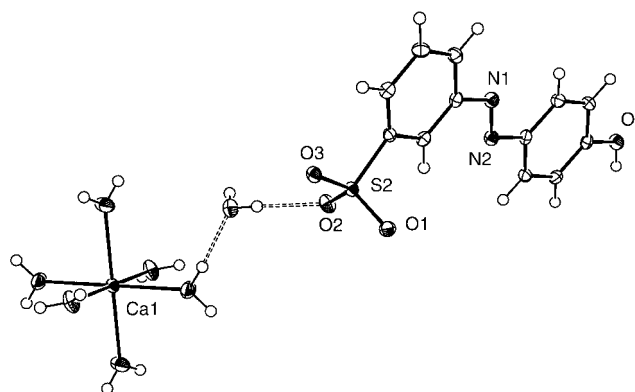Figure 6. The ladder structure formed by **Li3**.

Figure 7. Only when the position of the SO₃ group is changed from *para* to *meta* are some Ca compounds found to have solvent-separated ion-pair structures, illustrated by **Ca8**.

the inorganic core of its neighbouring chains (thus creating the alternating organic–inorganic layering).

Examination of Figures 4 and 6 show how these "tail" hydrogen-bonding interactions can occur through "tails" interpenetrating between the illustrated dye molecules. The one-sided distribution of azo ligands in **Ba3** leads to a subtle difference in chain packing from the other systems studied. Here the inorganic layers are twice the thickness, as each chain lies back-to-back with a neighbour so that the hydrophilic sides link through hydrogen bonding.

Ca complexes of *meta*-sulfonated azo dyes—changing supramolecular class by changing the SO₃ position: All the Ca salts of the *para*-sulfonated ligands are class 2 structures, but, as Table 1 shows, of the four *meta*-sulfonated species, two are not. These instead form class 1 solvent-separated ion pairs. See Figure 7 for an illustration of **Ca8**. It seems evident that the *meta*-ligands are less attractive to Ca than the *para*-ligands, and that this leads to Ca favouring solvation by water in some cases. Even in the class 2 structure of **Ca10** (Figure 3), only the minimum η^1, μ_1 metal-to-SO₃ interaction is seen. These observations tally neatly with the classic push–pull mechanism illustrated in colourants textbooks.[17] The colour of azo dyes is often explained by a resonance mechanism controlled by an electron-donating group on one side of the azo group and an electron-withdrawing group on the other. In the model azo dyes used in this study, the electron-donating groups are R and R′ and the (weakly) electron-withdrawing group is SO₃ (Table 1). In the *para*-sulfonated ligands, the electron-donating groups

push electron density through to the SO₃ group, but the *meta*-sulfonates are not conjugated to the R donors. It is possible that this results in a small decrease in electron density at the *meta*-SO₃ and that this is responsible for changing the coordination behaviour of the ligands. In support of an electronic explanation for this, **Ca10** forms a Ca–SO₃ bond whereas **Ca8** and **Ca9** do not. Complex **Ca10** has a much stronger electron-donating group (an amine) than the others (OH).

Structural type 3, M–SO₃-bonded complexes with higher connectivities—cages and sheets: The heavier Group 1 metals (Na, K and Rb) also have structures based around metal-to-sulfonate bonding. However, several factors combine to give more complex networks than those observed for Li and the Group 2 metals. The Group 1 metals have a higher metal/ligand ratio than those of the Group 2 metals (1:1 compared to 1:2), whilst Na, K and Rb as a group typically have much higher coordination numbers than Li. Thus, from the simplest principles, the networks formed by Na, K and Rb should be more complex than those formed by the Group 2 metals (as there are twice as many nodes per azo group) and also more complex than the Li networks (as each individual node will make many more connections). The most complicated motifs seen for the class 2 compounds are one-dimensional chains of rings or ladders (e.g., **Li3**, **Ca1** or **Ca11**, below). With extra contacts, these motifs can expand in a number of ways. Chains of rings can link togeth-

er to form two-dimensional sheets of rings, extra "capping" or bridging interactions can transform the one-dimensional chain of rings into a one-dimensional chain of cages and these can in turn link to give two-dimensional sheets of cages. All of these structural types have been observed. **K2** forms a one-dimensional coordination polymer of the chain-of-cages type (Figure 8), as does **Na1**.[1] However, **Na2**
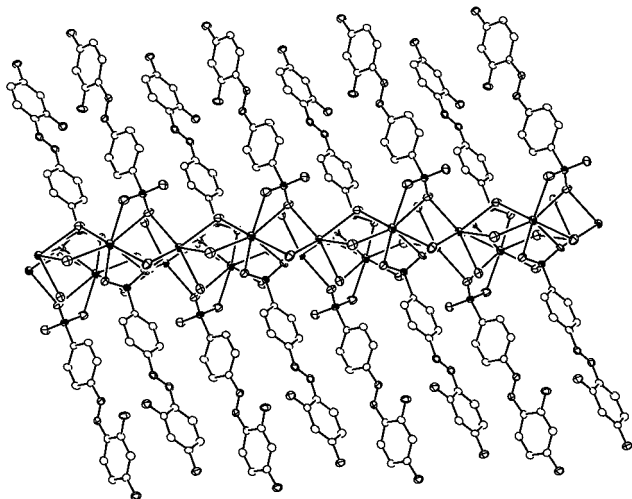

Figure 8. The structure of **K2** forms a one-dimensional coordination polymer with a more complex series of ligand-to-metal bridges than those found for Ca, Ba and Li structures.

forms instead a two-dimensional sheet made from interlocking 8- and 12-membered rings (Figure 9a),[1] illustrating again how difficult it is to predict the detailed behaviour of a given species. Figure 9b shows the structure of **Rb3**—a typical two-dimensional sheet of cages with bridging water ligands linking chains of cages. In comparison to the class 2 structures formed by Li, Ca and Ba, the sulfonates of the class 3 structures of Na, K and Rb tend to have a higher hapticity (0–3, with 2 and 3 the most common, whilst only Li ever has a hapticity of 3 in the class 2 structures). In addition, the class 3 structures tend to bridge more metals (maximum five for class 3 compared to maximum three for class 2 structures, and then only for Li, Table 3). The definitive differences are, however, that all class 3 structures feature bridging sulfonates and all class 3 hydrates have bridging water ligands.

Na4—an exception to the rules: Of the 43 structures of s-block salts of *para*- and *meta*-sulfonated azo dyes investigated, only one does not fit into the class structure proposed. This exception, **Na4**, essentially forms a solvent-separated ion-pair system complicated to some extent by the cationic part forming a one-dimensional polymer through Na–water bridging (Figure 10). For a *para*-sulfonated ligand such as **4**, we predict that only Mg salts should form such structures. Examining Tables 1 and 2 shows that **4** is slightly atypical as its tail NMe_2 group is unlikely to take part in hydrogen bond formation—unlike the other tails, which mostly contain OH or NH_2 groups. This may affect the packing of the
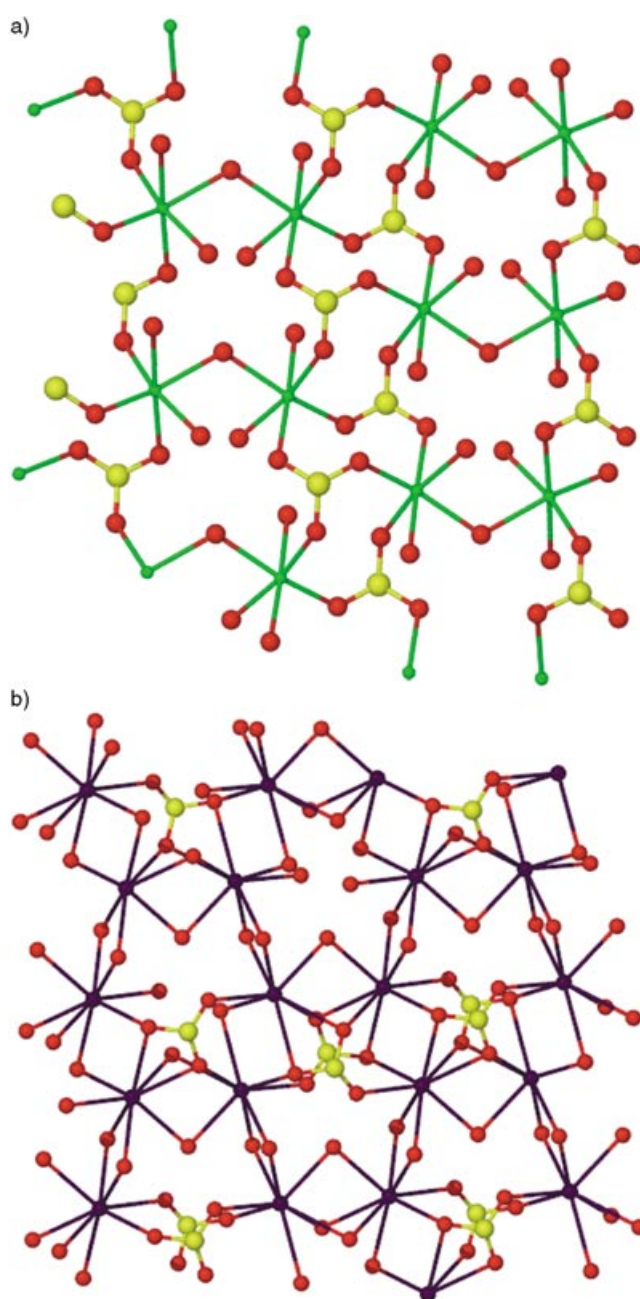

Figure 9. a) The inorganic portion of the structure of **Na2** showing the two-dimensional sheet formed by linking chains of rings.[1] Green = Na, Yellow = S, Red = O. b) The two-dimensional coordination network of **Rb3** with the C, N and H atoms removed for clarity. Rb = purple, O = red, S = yellow.

azo ligands and partly explain this unpredictable behaviour. Interestingly, one of the few relevant literature structures available is of an ethanol/water solvate of **Na4**.[12] This forms the expected class 3 structure with a two-dimensional coordination polymer. Furthermore, on recrystallising **Na4** from methanol, we isolated a methonolate structure that is also of the class 3 type (Figure 11), although here the lack of bridging water favours a one-dimensional "chain-of-cages" motif. It seems that in the competition reaction between solvent and azo ligand, water unexpectedly predominates from aqueous solution and forms a solvent-separated species,
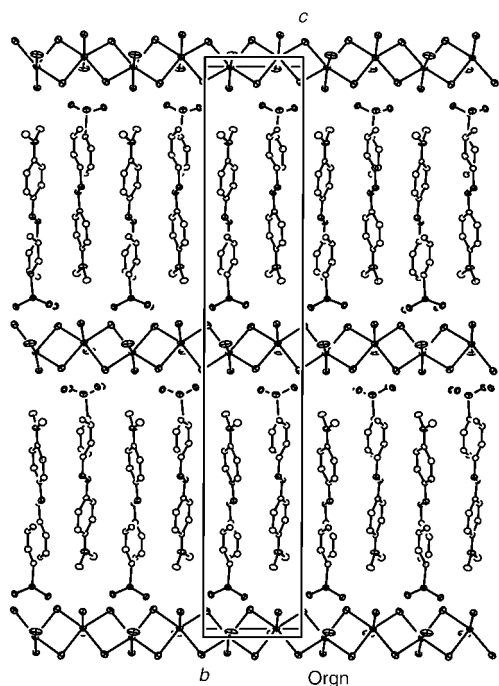
Figure 10. Packing diagram viewed along the *a* direction and showing that the organic and inorganic layers of **Na4** interact only through hydrogen bonding.
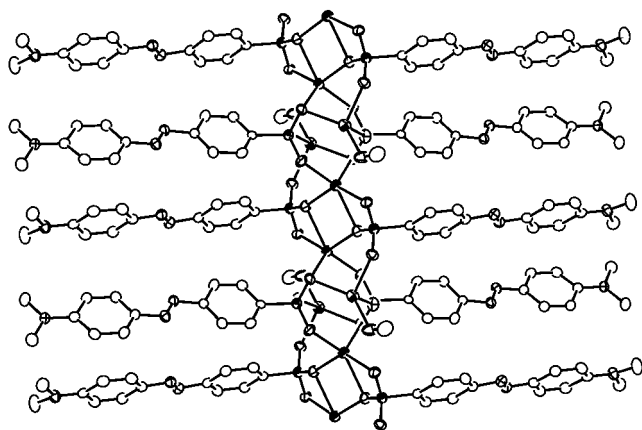

Figure 11. When crystallised from MeOH, **Na4** has the expected class 3 structure.

whereas the weaker ligands methanol and ethanol allow ligation by the dye molecules and the expected class 3 structural form.

Structural trends and metal properties: In their work on alkaline earth metal compounds of 4,5-dihydroxybenzene-1,3-disulfonate (**12**),[7a] Côté and Shimizu report on an intriguing series of compounds in which, as here, the Mg species forms a zero-dimensional solvent-separated ionic solid, but the Ca, Sr and Ba species form one-, two- and three-dimensional coordination polymers, respectively. This change in dimensionality is based on two trends: Moving down Group 2, the metals form fewer bonds with water and more with SO_3 groups. The authors rationalise this with reference to hard–

soft acid–base principles, which works well if SO_3 is described as a soft base. The sulfonated-azo coordination polymers presented here tend towards lower dimensionalities than does **12**, presumably due to the comparatively large size of the organic fragments and their lower concentration of metal-binding groups. However, the same trends of higher dimensionality, more SO_3 contacts and less water-binding with progression down the periodic table are generally observed (Table 3). Allowing for the typical slightly anomalous behaviour of Li, these trends can again be related to polarizability (and hence hard- or softness) within each periodic group, but this fails to explain differences between the groups. For instance, Ba^{2+} is more polarizable than K^+, but makes more water contacts and fewer SO_3 contacts than K. An alternative explanation can be based on electronegativities as an expression of "ionic character". Examination of Table 3 shows that the three proposed classes of structure follow exactly the trends in electronegativity (class 1: Mg 1.293; class 2: Ca, Ba, Li 1.034–0.881; class 3: Na, K, Rb 0.869–0.706), with the most electronegative class 2 metal Ca being persuaded to adopt class 1 structures by use of the appropriate ligand. As the most electronegative and hence most covalent metal used, Mg forms the strongest bonds with water. As the metals become more ionic in character, they form weaker interactions with all Lewis bases, but the ionic character of the M-to-SO_3^- interaction is increasingly favoured over M-to-OH_2 interactions.

Application of classifications to more complex colourants: As stated earlier, a prime test of this work is to successfully apply the rules and observations made on our small model compounds to larger compounds more representative of those used in the dye and pigment industries. However, there is a shortage of known structures for these common dyestuff types. A search of the Cambridge Structural Database[18] for structures with aromatic rings on either side of an azo linkage found no relevant *para*-sulfonated structures and only one of the *meta*-sulfonated type.[6c] The *meta* species is a Ca salt of Congo Red (C.I. 22120, Direct Red 28), which was crystallised from ethylene glycol. This does give a class 1 solvent-separated ion pair, as found for the model *meta* species, but using the good chelating ligand ethylene glycol to achieve this positive result must introduce bias to some extent. Previously, we had success in growing crystals of chlorinated derivatives of the toner pigment Ca4B (CIPR 57:1) from DMF.[8] These are sulfonated azo species, but the sulfonate is *ortho* to the azo unit and additionally is situated so as to form a chelating system with the keto and carboxylate groups also present. It was thus decided to synthesise a *meta* isomer of these pigments (**11**) that would be relevant to this study. As can be seen in Figure 12, a structure of **Ca11** was obtained. This is not only a class 2, one-dimensional chain of rings as expected, but in fact also has a supramolecular motif strictly analogous to that of the model dye **Ca1**.[1] Thus, despite the evident differences between the small model dyes and the larger, more complex colourants, (e.g., presence of larger organic fragments, such as napthalenes and biphenyls, polyazo rather than monoazo units, multiple acid groups for metal binding, adoption of
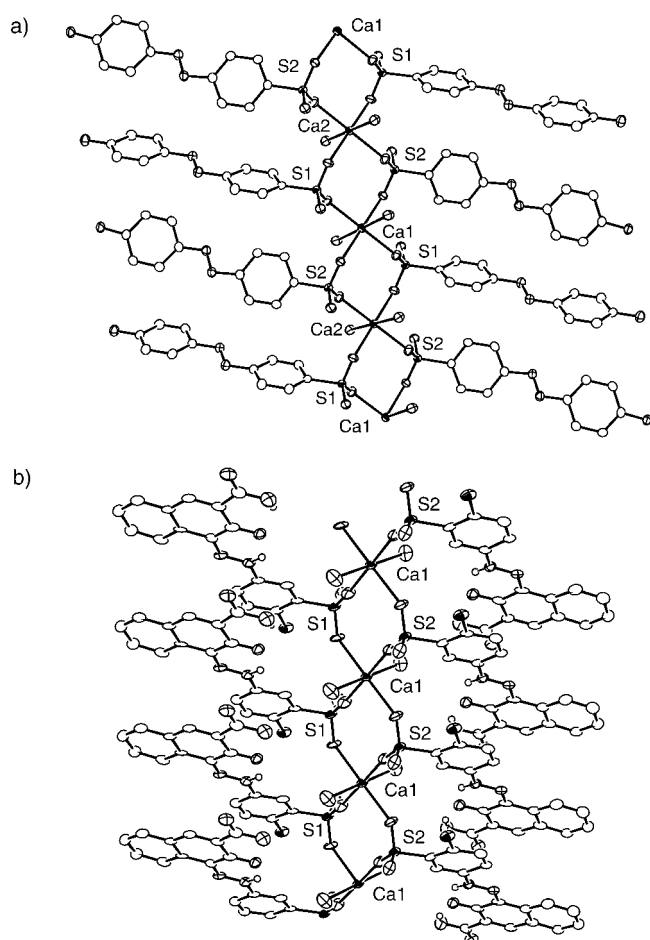
a)

b)

Figure 12. The one-dimensional "chain-of-ring" structures of a) **Ca1** and b) **Ca11**, both of which are based on eight-membered (CaOSO)$_2$ rings and octahedral Ca centers with two terminal and mutually *trans* solvent ligands.

the keto–hydrozone form rather than the simple azo form and use of nonaqueous solvents), the available examples of structures of complex sulfonated azo colourants are successfully modelled by the structures of the smaller dyes.

Conclusion

Prior to this study, only six crystal structures of s-block metal salts of simple sulfonated azo dyes were known.[1,12] We have now expanded this series to 43 structures. With the large amount of structural information now available, it is possible to classify the previous, seemingly random variety of coordination networks formed. All form structures with alternating organic and inorganic layers, but these may be divided into three classes. Metal type largely governs which class of structure is formed and this can be understood by considering the interplay of the basic factors governing s-block metal coordination, that is, charge, size and hence electronegativity. For *para*-sulfonated azo dyes, Mg compounds form solvent-separated ion-pair solids with no interactions between the metal and the SO$_3$ group; Ca, Ba and Li form simple zero- or one-dimensional structures with

metal-to-SO$_3$ bonds and terminal solvent ligands; and Na, K and Rb form more complex coordination polymers (reminiscent of mineral-type structures as opposed to the more molecular-appearing structures of the other metals) with generally more metal-to-SO$_3$ contacts per ligand and with water molecules bridging metals. This does not mean that the metal is the only influence on the structure formed. The ability to change structural type systematically is shown by a decrease in the number of Ca-to-SO$_3$ contacts found on moving the sulfonate to the *meta*-position—indeed in two cases this decrease leads to a change in structural class and solvent-separated ion-pair solids with no metal-to-SO$_3$ contacts formed. The ligand substituents also have more subtle (and seemingly random) effects on the details of the structures observed. For instance, both **Na1** and **Na2** form class 3 structures, but **Na1** is a one-dimensional chain of cages, whilst **Na2** is a two-dimensional sheet. Thus, although the types of interactions and broad structural class can be predicted, the exact detail of the structure formed cannot. Of the 43 simple model structures studied, 42 comply with the classifications described. Part 2 of this study will be published separately and will describe the increased complexity observed following the introduction of a second metal-bonding group to the dyes; however, the basic structures described here also hold for these species. The one exception is **Na4**, which unexpectedly forms a solvent-separated species when crystallised from aqueous solution, but forms the expected structural types when crystallised from methanol or ethanol. We have also examined and expanded the limited available data on more complex colourants and have shown that despite their inherent chemical differences, these compounds also fit easily into our classification system. This observation is important, as the identification of structure–property relationships (properties of particular interest being colour, solubility and habit) must be applicable to modern, industrial colourants as well as to simpler species.

Experimental Section

General: Dyes **1–11** were synthesised by variations on the well-known diazonium coupling reaction.[10] The synthesis of the Na salt of **11** is given as an example. The main variation for the other dyes is that those with amine substituents were synthesised under slightly acidic conditions in the presence of glacial acetic acid. IR spectra were recorded as KBr discs, Raman spectra were recorded from solid placed on microscope slides.

Synthesis of Na11: 2-Chloro-5-aminobenzene sulfonic acid (3.04 g, 14.66 mmol) was added to sodium carbonate (0.82 g, 7.78 mmol) in water (50 mL). This solution was added to ice (40 g), and then sodium nitrite (1.10 g, 15.97 mmol) in water (20 mL) was added. This solution was then

Table 4. Selected crystal parameters and refinement data.

	Mg1	Ca2	K2	Li3	Rb3	Ba3
formula	$[Mg(H_2O)_6][\mathbf{1}]_2\cdot 2H_2O$	$[Ca(\mathbf{2})_2(H_2O)_5]H_2O$	$[K(\mathbf{2})(H_2O)_2]$	$[Li(\mathbf{3})(H_2O)]$	$[Rb(\mathbf{3})(H_2O)_{1.5}]$	$[Ba(\mathbf{3})_2(H_2O)_6]$
M_R	722.98	734.72	368.40	299.23	388.78	798.02
crystal system	monoclinic	monoclinic	triclinic	monoclinic	monoclinic	monoclinic
space group	$P2_1/c$	$P2_1/n$	$P\bar{1}$	$P2_1/n$	$C2/c$	$P2/c$
a [Å]	11.7322(3)	7.9944(2)	8.1774(6)	5.3520(1)	35.2556(10)	13.3848(2)
b [Å]	7.1505(3)	10.7236(2)	10.5289(8)	7.9210(1)	7.7380(2)	6.3152(1)
c [Å]	37.0550(14)	34.9746(6)	17.4832(13)	31.2980(4)	10.6741(4)	36.2265(7)
α [°]	90	90	89.820(2)	90	90	90
β [°]	96.427(2)	94.6230(1)	85.488(2)	92.229(1)	99.883(1)	92.1150(1)
γ [°]	90	90	86.811(2)	90	90	90
V [Å³]	3089.05(19)	2988.57(11)	1498.30(19)	1326.52(2)	2868.76(15)	3060.06(9)
Z	4	4	4	4	8	4
ρ_{calcd} [Mg m⁻³]	1.555	1.633	1.633	1.498	1.800	1.732
μ [mm⁻¹]	0.275	0.435	0.533	0.262	3.621	1.506
T [K]	123	123	150	123	123	123
λ [Å]	0.71073	0.71073	0.6880	0.71073	0.71073	0.71073
reflns collected	13146	16813	14026	5579	18463	55611
unique reflns	7064	8703	7125	3006	3285	8180
R^{int}	0.0379	0.0303	0.0354	0.0184	0.0659	0.1050
GoF	1.047	1.025	0.854	1.238	1.102	0.959
$R[I>2\sigma(I)]$	0.0415	0.0362	0.0419	0.0370	0.0503	0.0339
wR	0.1250	0.0912	0.0916	0.1212	0.1250	0.0690

	Na4	Na4′	Mg8	Ca8	Ca10	Ca11
formula	$[Na(H_2O)_4][\mathbf{4}]$	$[Na(\mathbf{4})(MeOH)_{0.5}]$	$[Mg(H_2O)_6][\mathbf{8}]_2\cdot 2H_2O$	$[Ca(H_2O)_6][\mathbf{8}]_2\cdot 2H_2O$	$[Ca(\mathbf{10})_2(H_2O)_4]\cdot 4H_2O$	$[Ca(\mathbf{11})_2(dmf)_{1.55}(H_2O)_{0.45}]$
M_R	399.40	343.35	722.98	738.75	913.00	977.54
crystal system	monoclinic	monoclinic	triclinic	triclinic	monoclinic	monoclinic
space group	$P2_1/c$	$P2_1/n$	$P\bar{1}$	$P\bar{1}$	$P2_1/c$	$P2_1$
a [Å]	6.1073(4)	11.0265(2)	6.7060(2)	6.8325(1)	8.4297(1)	17.9160(15)
b [Å]	7.0736(4)	7.9870(2)	7.0020(2)	7.0714(1)	7.9176(1)	5.5834(5)
c [Å]	41.782(3)	35.8318(8)	18.3500(5)	18.6064(5)	31.7760(4)	21.986(22)
α [°]	90	90	93.273(1)	92.754(1)	90	90
β [°]	91.198(2)	95.653(1)	93.661(1)	92.930(1)	96.864(1)	90.222(2)
γ [°]	90	90	114.788(2)	116.172(1)	90	90
V [Å³]	1804.6(2)	3140.31(12)	777.30(4)	803.25(3)	2105.62(5)	2171(2)
Z	4	8	1	1	2	2
ρ_{calcd} [Mg m⁻³]	1.470	1.452	1.545	1.527	1.440	1.495
μ [mm⁻¹]	0.246	0.254	0.273	0.405	0.325	0.437
T [K]	123	123	123	123	123	150
λ [Å]	0.71073	0.71073	0.71073	0.71073	0.71073	0.6892
reflns collected	10788	11753	6717	6432	15769	11092
unique reflns	3759	6137	3530	3389	4671	5710
R^{int}	0.0908	0.0908	0.0354	0.0214	0.0634	0.0454
GoF	1.033	1.008	1.033	1.034	0.980	0.942
$R[I>2\sigma(I)]$	0.0583	0.0531	0.0397	0.0292	0.0402	0.0577
wR	0.1530	0.1104	0.0981	0.0726	0.0981	0.1469

slowly added to concentrated HCl (5 mL) on ice (50 g), giving a cream precipitate. The temperature was maintained below 5°C at all times by the addition of ice. β-Oxynaphthanilic acid (3.16 g, 17.92 mmol) was prepared as a basic solution, pH 9, by using sodium carbonate. The diazonium suspension was added slowly to this with the immediate formation of a bright red precipitate. After stirring for 1 hour, solid **Na11** was collected by filtration and air dried, yield 64%. **Ca11** was obtained by adding a slight excess of $CaCl_2$ to an aqueous solution of **Na11**. After stirring for 1 hour the **Ca11** precipitate was recovered by filtration, yield 66%.

Data for [Mg(OH₂)₆][1]₂·2H₂O]: IR: $\tilde{v}=3395, 3170, 3042, 2847, 1597, 1495, 1423, 1182, 1034$ cm⁻¹; Raman: $\tilde{v}=1120, 1146, 1436$ cm⁻¹ (masked by fluorescence); DSC: endothermic 116, 140, 205°C; exothermic 352, 382°C.

Data for [Ca(2)₂(OH₂)₅]·H₂O: IR: $\tilde{v}=3457, 1936, 1598, 1506, 1419, 1332, 1219, 1116, 1034, 927$ cm⁻¹; Raman: $\tilde{v}=1045, 1126, 1163, 1197, 1322, 1375, 1420, 1591$ cm⁻¹.

Data for [K(2)(OH₂)₂]: IR: $\tilde{v}=3472, 3390, 1593, 1469, 1372, 1198, 1121, 1039, 839, 803$ cm⁻¹; Raman: $\tilde{v}=1033, 1122, 1161, 1198, 1326, 1374, 1418, 1592$ cm⁻¹; DSC: endothermic 115°C; exothermic 315°C.

Data for [Li(3)OH₂)]: IR: $\tilde{v}=1589, 1506, 1429, 1398, 1255, 1183, 1122, 1045, 1004, 850, 707$ cm⁻¹; Raman: $\tilde{v}=1126, 1146, 1192, 1394, 1434, 1460$ cm⁻¹; DSC: endothermic 175°C; exothermic 390°C.

Data for [Rb(3)(OH₂)₁.₅]: IR: $\tilde{v}=1639, 1454, 1372, 1214, 1168, 1116, 1024, 1004$ cm⁻¹; Raman: $\tilde{v}=1125, 1157, 1431$ cm⁻¹ (masked by fluorescence); DSC: endothermic 94, 115°C; exothermic 352°C.

Data for [Ba(3)₂(OH₂)₆]: IR: $\tilde{v}=3421, 2709, 1654, 1454, 1367, 1295, 1157$ cm⁻¹; Raman: $\tilde{v}=1125, 1152, 1195, 1400, 1431, 1459, 1595$ cm⁻¹; DSC: endothermic 95°C; exothermic 388°C.

Data for [Na(OH₂)₄][4]: IR: $\tilde{v}=3472, 2914, 1608, 1378, 1188, 1116, 1029, 814$ cm⁻¹; Raman: $\tilde{v}=1115, 1141, 1198, 1315, 1365, 1389, 1424, 1586$ cm⁻¹; DSC: endothermic 72, 78, 86, 106°C; exothermic 212, 300°C.

Data for [Na(4)(HOMe)₀.₅]: IR: $\tilde{v}=1675, 1650, 1603, 1516, 1424, 1368, 1163, 1117, 1030, 999, 851, 820, 697, 569$ cm⁻¹; Raman: $\tilde{v}=1112, 1140, 1195, 1363, 1389, 1411, 1421, 1586$ cm⁻¹.

Data for [Mg(OH₂)₆][8]₂·2H₂O: IR: $\tilde{v}=3057, 1602, 1500, 1198, 1034$ cm⁻¹; Raman: masked by fluorescence; DSC: endothermic 118, 219, 252°C; exothermic 385°C.

Acknowledgement

[1] A. R. Kennedy, M. P. Hughes, M. L. Monaghan, E. Staunton, S. J. Teat, W. E. Smith, *J. Chem. Soc. Dalton Trans.* **2001**, 2199.

[2] a) D. Braga, F. Grepioni, G. R. Desiraju, *Chem. Rev.* **1998**, *98*, 1375; b) K. W. Henderson, A. R. Kennedy, L. Macdonald, D. J. MacDougall, *Inorg. Chem.* **2003**, *42*, 2839; c) W. S. Sheldrick, *J. Chem. Soc. Dalton Trans.* **2000**, 2041; d) H. Bock, J.-M. Lehn, J. Pauls, S. Holl, V. Krenzel, *Angew. Chem.* **1999**, *111*, 1004; *Angew. Chem. Int. Ed.* **1999**, *38*, 952.

[3] See, for example: a) A. J. Blake, N. R. Champness, P. Huberstey, W.-S. Li, M. A. Withersby, M. Schröder, *Coord. Chem. Rev.* **1999**, *183*, 117; b) M. J. Plater, M. R. St. J. Foreman, T. Gelbrich, S. J. Coles, M. B. Hursthouse, *J. Chem. Soc. Dalton Trans.* **2000**, 3065; c) P. J. Strang, B. Olenyuk, *Acc. Chem. Res.* **1997**, *30*, 502; d) S.-P. Yang, X.-M. Chen, L.-N. Ji, *J. Chem. Soc. Dalton Trans.* **2000**, 2337.

[4] a) Z. Hao, A. Iqbal, *Chem. Soc. Rev.* **1997**, *26*, 203; b) C. P. Price, A. L. Grzesiak, J. W. Kampf, A. J. Matzger, *Cryst. Growth Des.* **2003**, *3*, 1021; c) R. M. Vrcelj, E. E. A. Shepherd, C. Yoon, J. N. Sherwood, A. R. Kennedy, *Cryst. Growth Des.* **2002**, *2*, 609; d) N. B. McKeown, *Phthalocyanine Materials: Synthesis, Structure and Function*, Cambridge University Press, Cambridge, **1988**.

[5] H. G. Brittain, *Polymorphism in Pharmaceutical Solids*, Dekker, New York, **1999**.

[6] a) K. Ishii, W. E. Klunk, S. Arawaka, M. L. Debnath, Y. Furiya, N. Sahara, S. Shoji, A. Tamaoka, J. W. Pettegrew, H. Mori, *Neurosci. Lett.* **2002**, *333*, 5; b) W. G. Turnell, J. T. Finch, *J. Mol. Biol.* **1992**, *227*, 1205; c) W. H. Ojala, C. R. Ojala, W. B. Gleason, *Antiviral Chem. Chemother.* **1995**, *6*, 25; d) W. H. Ojala, E. A. Sudbeck, L. K. Lu, T. I. Richardson, R. E. Lovrien, W. B. Gleason, *J. Am. Chem. Soc.* **1996**, *118*, 2131; e) C. C. Evans, L. Sukavto, M. D. Ward, *J. Am. Chem. Soc.* **1999**, *121*, 320.

[7] For recent work on coordination in s-block metal sulfonates see a) A. P. Côté, G. K. H. Shimizu, *Chem. Eur. J.* **2003**, *9*, 5361; b) S. A. Dalrymple, G. K. H. Shimizu, *Chem. Eur. J.* **2002**, *8*, 3010; c) A. P. Côté, G. K. H. Shimizu, *Coord. Chem. Rev.* **2003**, *245*, 49; d) J. Cai, C.-H. Chen, C.-Z. Liao, X.-L. Feng, X.-M. Chen, *Acta Crystallogr., Sect. B* **2001**, *57*, 520; e) G. Mezei, R. G. Raptis, *New J. Chem.* **2003**, *27*, 1399; f) J. L. Atwood, L. J. Barbour, M. J. Hardie, C. L. Raston, *Coord. Chem. Rev.* **2001**, *222*, 3.

[8] A. R. Kennedy, C. McNair, W. E. Smith, G. Chisholm, S. J. Teat, *Angew. Chem.* **2000**, *112*, 652; *Angew. Chem. Int. Ed.* **2000**, *39*, 638.

[9] a) S. S. De Silva, P. J. Camp, D. K. Henderson, D. C. R. Henry, H. McNab, P. A. Tasker, P. Wight, *Chem. Commun.* **2003**, 1702; b) A. M. Chippendale, G. McGeorge, R. K. Harris, C. M. Brennan, *Magn. Reson. Chem.* **1999**, *37*, 232; c) Y. Saito, B.-K. Kim, K. Machida, T. Uno, *Bull. Chem. Soc. Jpn.* **1974**, *47*, 2111; d) P. Savarino, G. Viscardi, E. Barni, R. Carpignano, A. L. Federov, *Dyes Pigm.* **1990**, *13*, 71.

[10] I. Szele, H. Zollinger, *Topp. Curr. Chem.* **1983**, *112*, 1.

[11] R. J. Cernik, W. Clegg, C. R. A. Catlow, G. Bushnell Wye, J. V. Flaherty, G. W. Greaves, I. Burrows, D. J. Taylor, S. J. Teat, M. Hamichi, *J. Synchrotron Radiat.* **1997**, *4*, 279.

[12] A. W. Hanson, *Acta Crystallogr., Sect. B.* **1973**, *29*, 454.

[13] A. Clearfield, *Prog. Inorg. Chem.* **1998**, *47*, 371.

[14] S. A. Dalrymple, M. Parvez, G. K. H. Shimizu, *Inorg. Chem.* **2002**, *41*, 6986.

[15] A. M. Jones, M. P. Lord, *Macmillan's Chemical and Physical Data*, Macmillan Press, London, **1992**, p 486.

[16] For a typical example see A. R. Kennedy, R. E. Mulvey, A. Robertson, *Chem. Commun.* **1998**, 89.

[17] See, for example: R. M. Christie, *Colour Chemistry*, RSC, Cambridge (UK), **2001**, pp. 26 – 44.

[18] F. H. Allen, *Acta Crystallogr., Sect. B* **2002**, *58*, 380.

[19] G. M. Sheldrick, SHELXL97, **1997**, University of Göttingen (Germany).

[20] J. B. Mann, T. L. Meek, L. C. Allen, *J. Am. Chem. Soc.* **2000**, *122*, 2780.

[21] *CRC Handbook of Chemistry and Physics*, 81st ed. (Ed.: D. R. Lide), CRC, Boca Raton, **2000**.